Electronic Supplementary Material (ESI) for Journal of Materials Chemistry A.

Supporting Information

Ordered mesoporous carbon supported $Ni_3V_2O_8$ composites for lithium-ion batteries with long-term and high-rate performance

Shiyao Lu, Tianxiang Zhu, Zhaoyang Li, Yuanchao Pang, Lei Shi, Shujiang Ding, Guoxin Gao

*

[*]Mr. S. Y. Lu, Mr. T. X. Zhu, Mr. Z. Y. Li, Miss. Y. C. Pang, Mr. L. Shi, Prof. S. J. Ding and Prof. G. X. Gao

Department of Applied Chemistry, School of Science, Xi'an Jiaotong University, Xi'an 710049, P. R. China

[*]*Corresponding authors:* gaoguoxin@mail.xjtu.edu.cn (G. X. Gao),

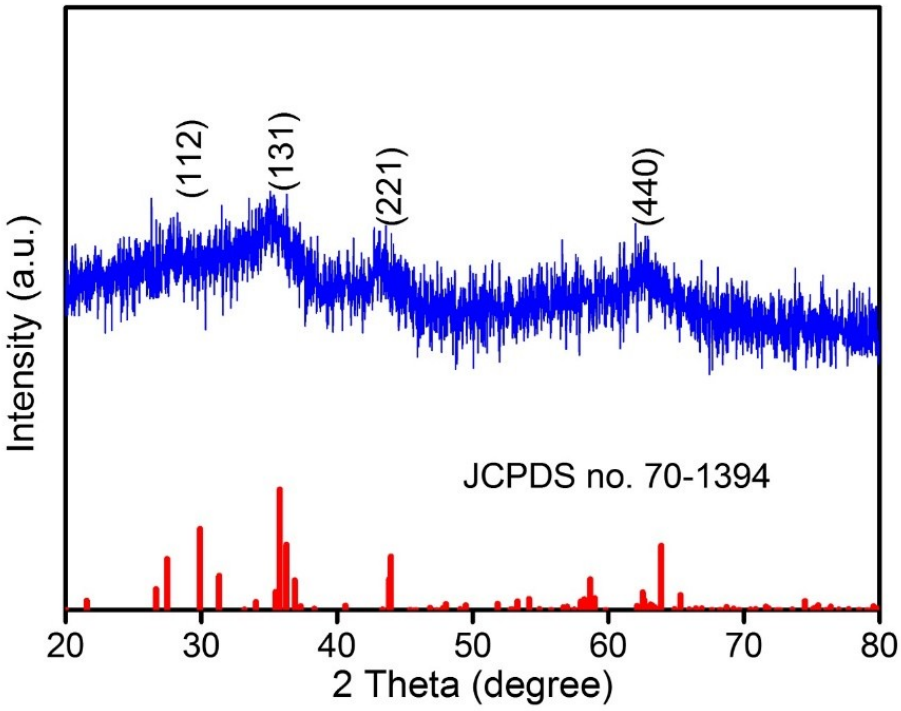

Figure S1. XRD pattern of the NiV-precusor@CMK-3.

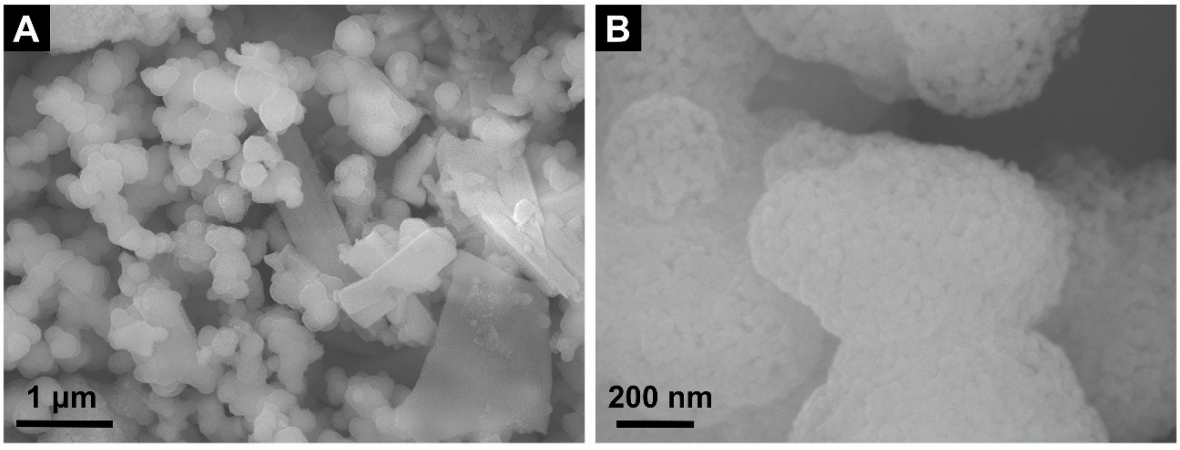

Figure S2. FESEM images of pristine $Ni_3V_2O_8$ aggregates.

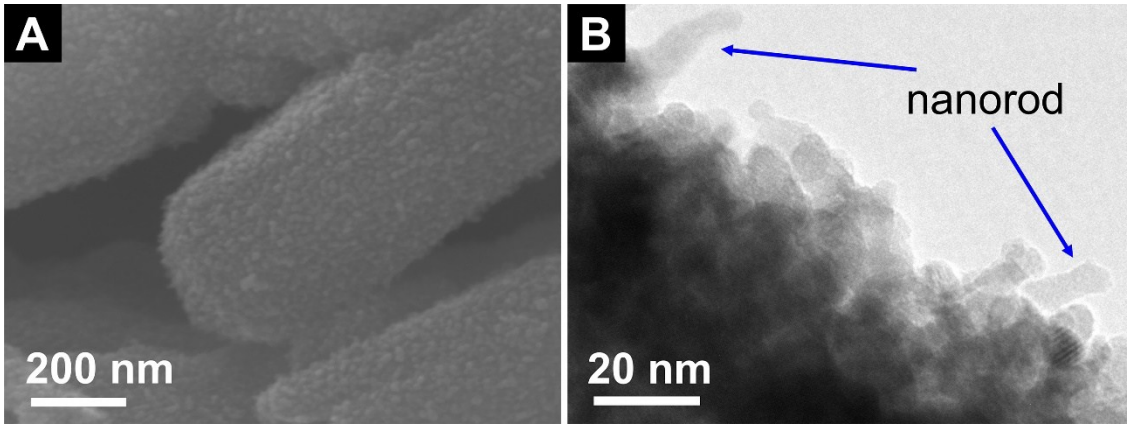

Figure S3. FESEM images (A) HRTEM images (B) of $Ni_3V_2O_8$@CMK-3 composites.

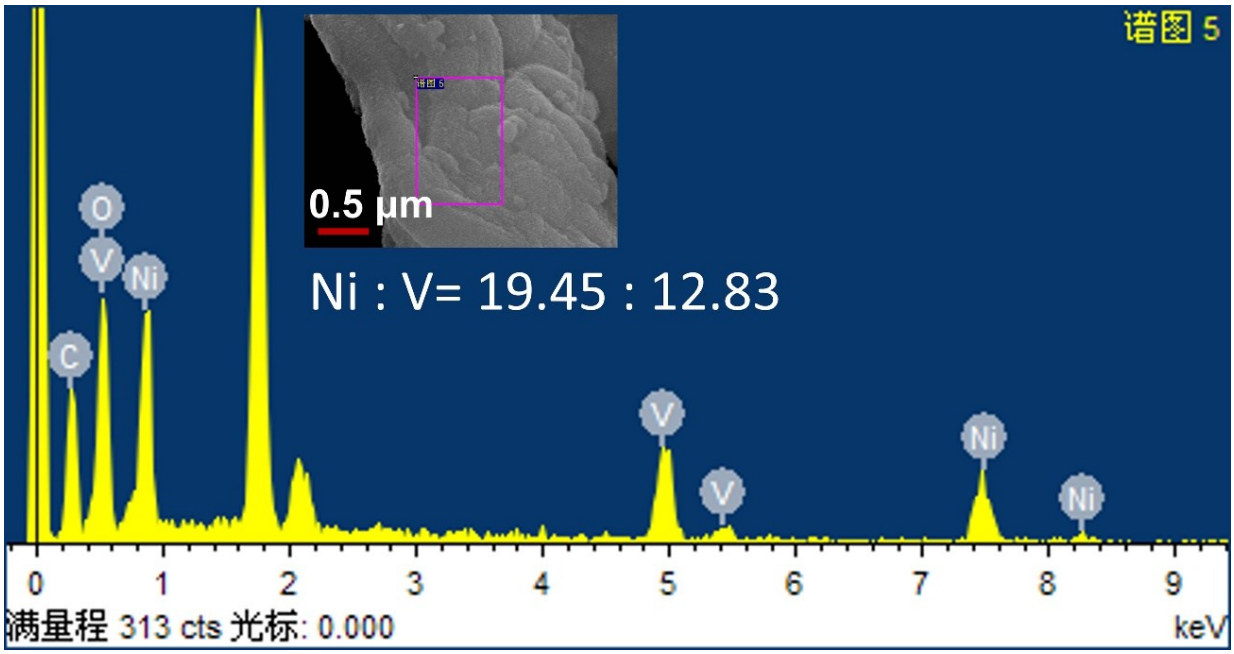

Figure S4. EDX pattern of as-prepared $Ni_3V_2O_8$@CMK-3 composites.

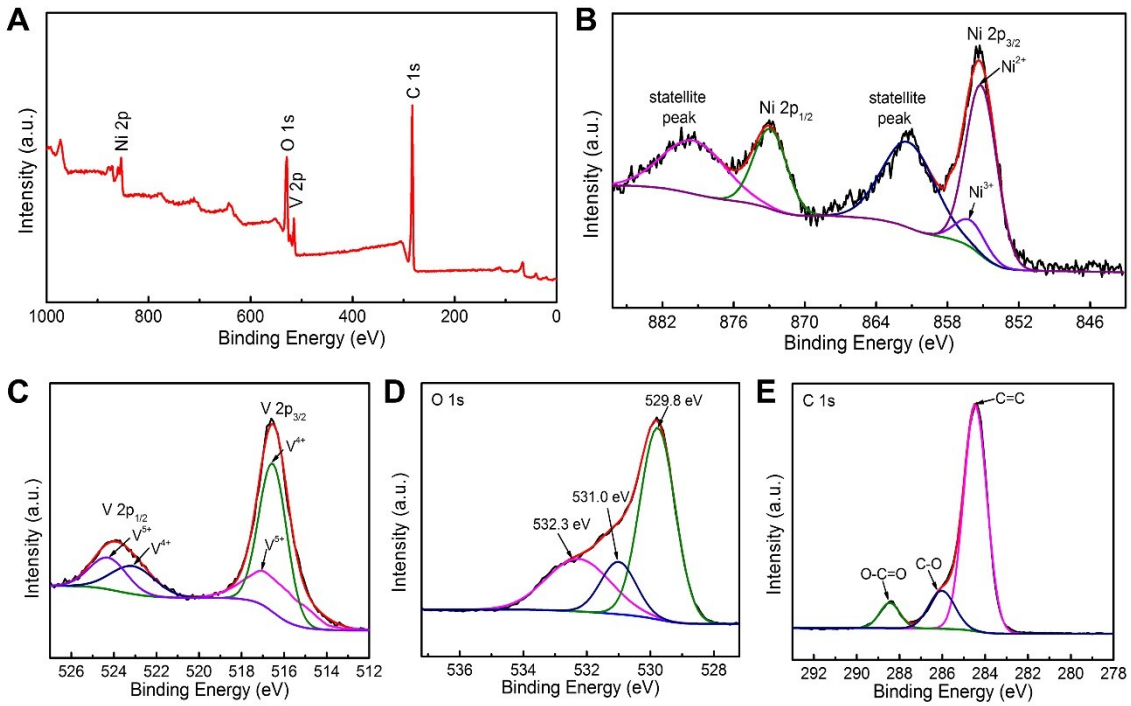

Figure S5. XPS spectra of as-prepared $Ni_3V_2O_8$@CMK-3 composites: (A) survey, (B) Ni 2p, (C) V 2p, (D) O 1s and (E) C 1s.

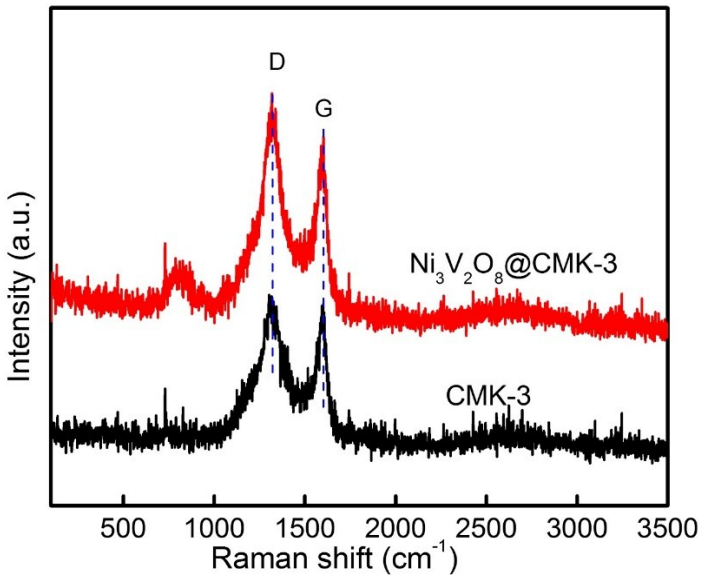

Figure S6. Raman spectroscopy of CMK-3 and the as-prepared $Ni_3V_2O_8$@CMK-3 composites.

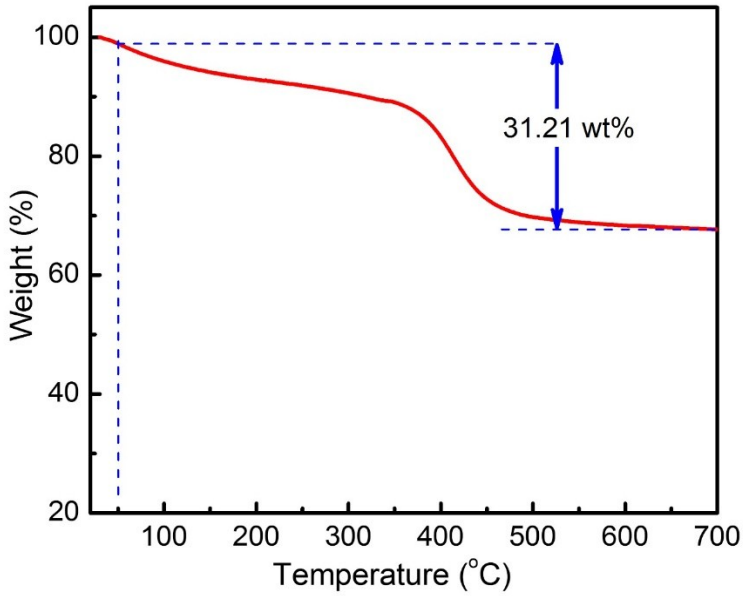

Figure S7. TGA curve of the as-prepared $Ni_3V_2O_8$@CMK-3 composites at a temperature ramp of 10 $^oC\ min^{-1}$

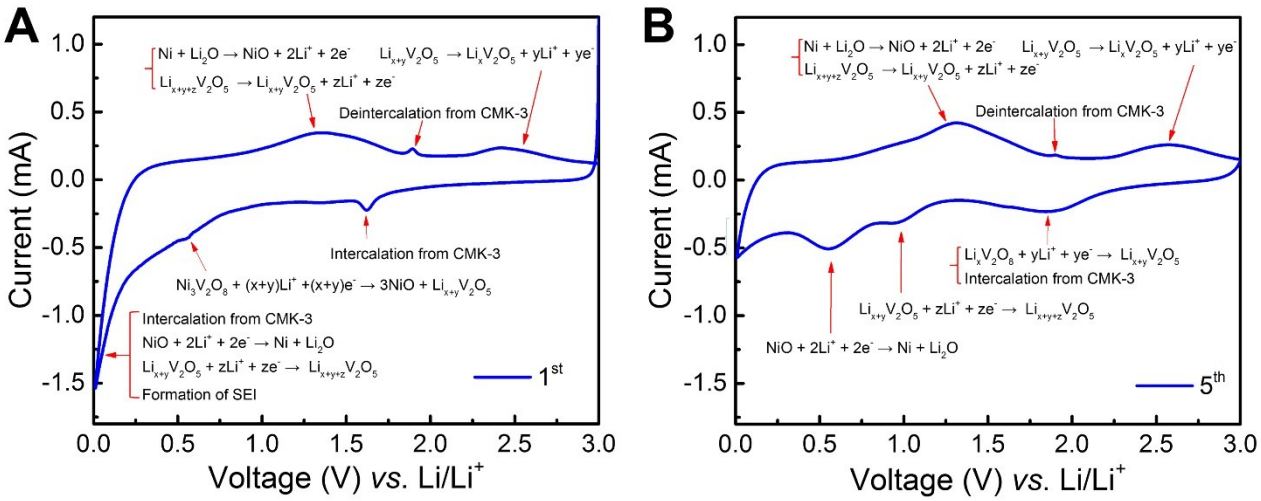

Figure S8. The possible electrochemical reactions between lithium ions and $Ni_3V_2O_8$@CMK-3 electrodes.

In the first cycle, the distinct reduction peaks mainly come from the continuous intercalation from CMK-3. The weak peak at 0.60 V is ascribed to the decomposition from $Ni_3V_2O_8$ to NiO. However, it disappears in the follow cycles due to the irreversible formation of a solid electrolyte interphase (SEI) and the decomposition of electrolyte. Subsequently such NiO further transforms into numerous metallic Ni quantum dots, scattering on the amporphous $Li_xV_2O_5$. In the subsequent cycles, as the activation of $Ni_3V_2O_8$, the reduction peaks form into three stable peaks. And the peak of intercalation from CMK-3 has been merged into the peak from the reaction: $Li_xV_2O_5 + yLi^+ + ze^- \rightarrow Li_{x+y}V_2O_5$. In summary, the possible reactions of electrodes that are shown in the following:

$Ni_3V_2O_8 + (x+y)Li^+ + (x+y)e^- \rightarrow 3NiO + Li_{x+y}V_2O_5$ (1)

$NiO + 2Li^+ + 2e^- \rightarrow Ni + Li_2O$ (2)

$Li_{x+y}V_2O_5 + zLi + ze^- \rightarrow Li_{x+y+z}V_2O_5$ (3)

Among these reactions, Reaction 1 is irreversible because the decomposition and deconstruction of the crystal structure of $Ni_3V_2O_8$.

The total reversible reaction is: $NiO + Li_xV_2O_5 + (y+z+2)Li^+ + (y+z+2)e^- \rightarrow Ni + Li_2O + Li_{x+y+z}V_2O_5$.

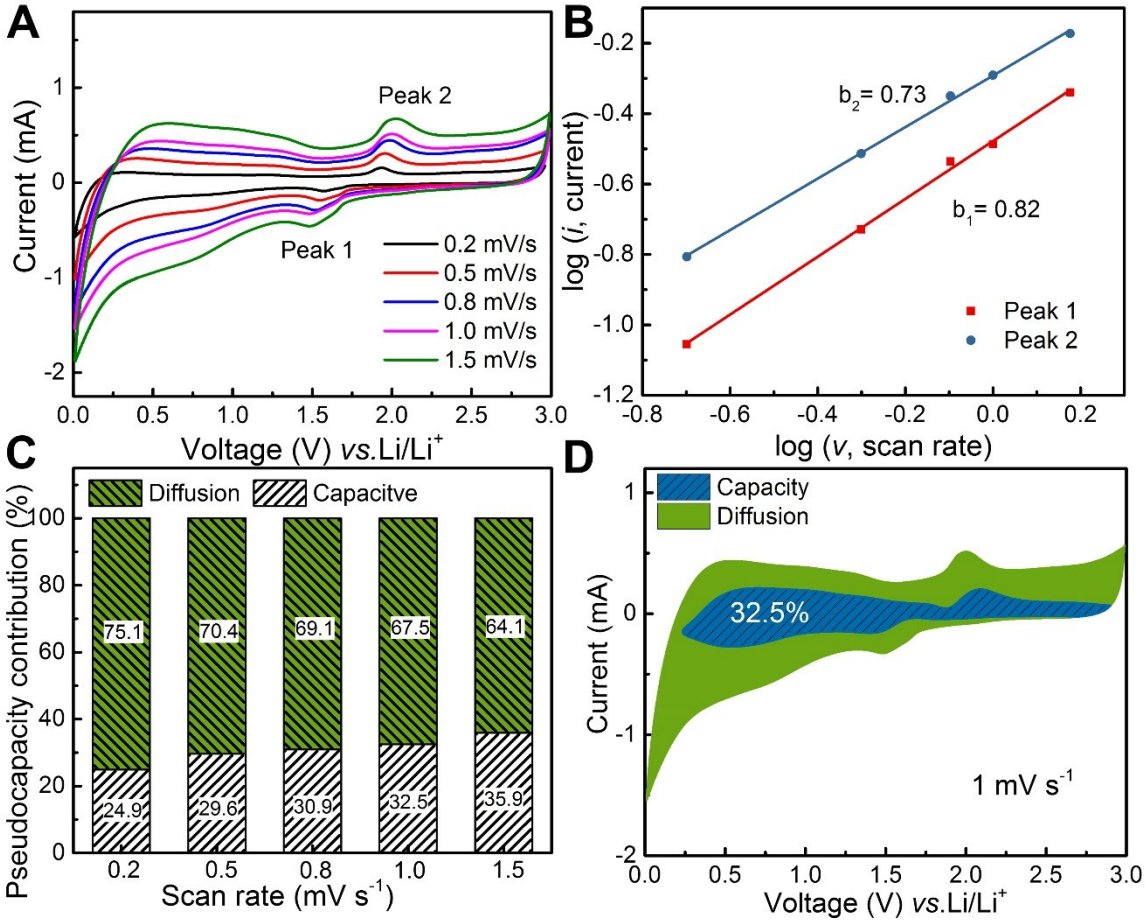

Figure S9. Pseudocapacitive behaviors of pure CMK-3 electrodes: (A) CV curves at different scan rates ranging from 0.2 to 1.5 mV s^{-1}; (B) corresponding log (*i*) *vs.* log (*v*) plots at each redox peak (*i*: peak current; *v*: scan rate); (C) bar chart showing the percent of pseudocapacitive contribution at different scan rates; and (D) CV curves with the pseudocapacitive fraction shown by the dark blue region at a scan rate of 1.0 mV s^{-1}.

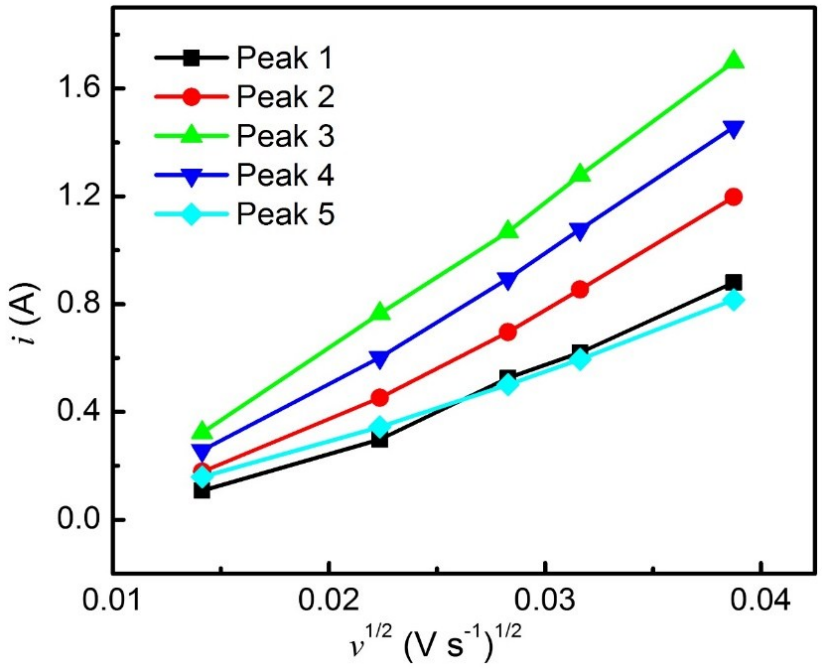

Figure S10. *i vs.* $v^{0.5}$ plots at each redox peak of CV curves of $Ni_3V_2O_8$@CMK-3 electrodes. (*i*: peak current; *v*: scan rate).

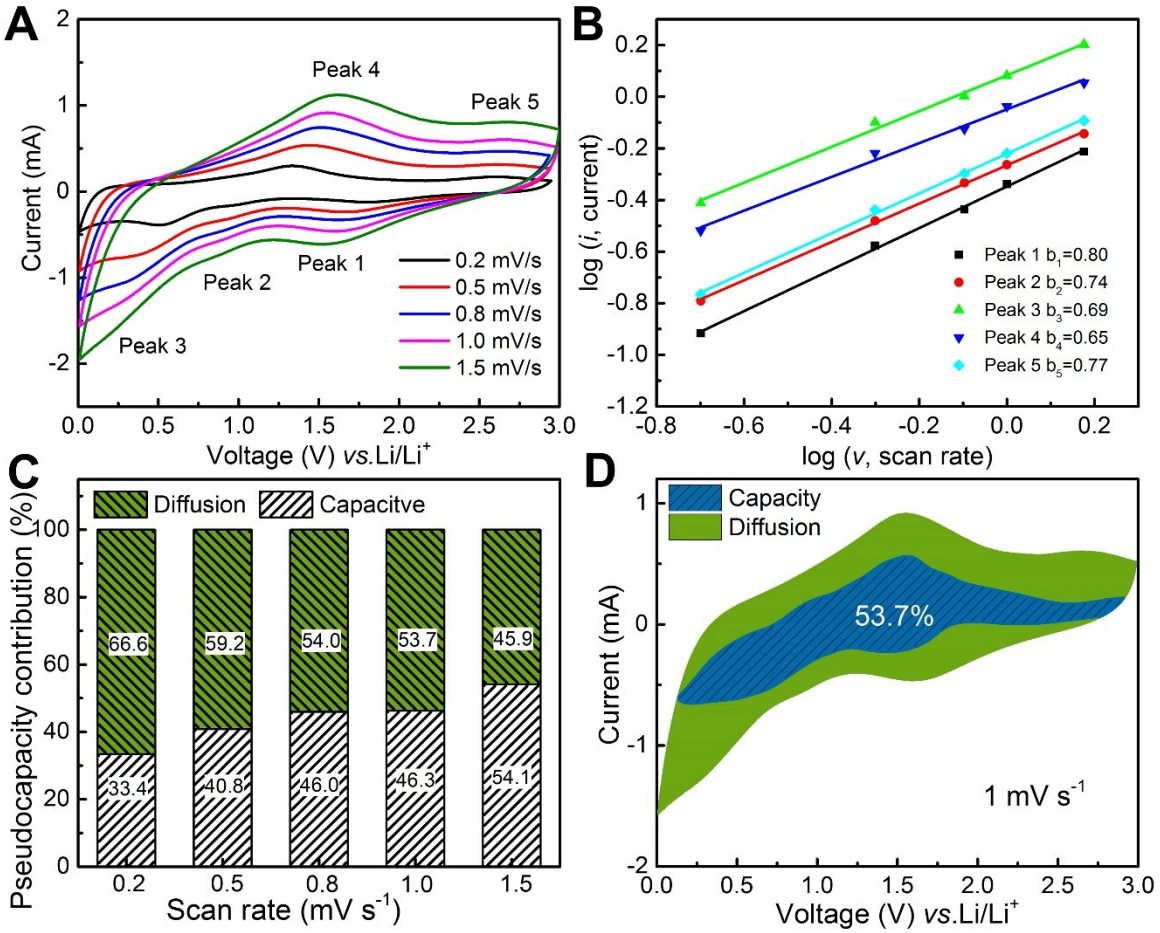

Figure S11. Pseudocapacitive behaviors of pure $Ni_3V_2O_8$ aggregates electrodes: (A) CV curves at different scan rates ranging from 0.2 to 1.5 mV s^{-1}; (B) corresponding log (*i*) *vs.* log (*v*) plots at each redox peak (*i*: peak current; *v*: scan rate); (C) bar chart showing the percent of pseudocapacitive contribution at different scan rates; and (D) CV curves with the pseudocapacitive fraction shown by the dark blue region at a scan rate of 1.0 mV s^{-1}.

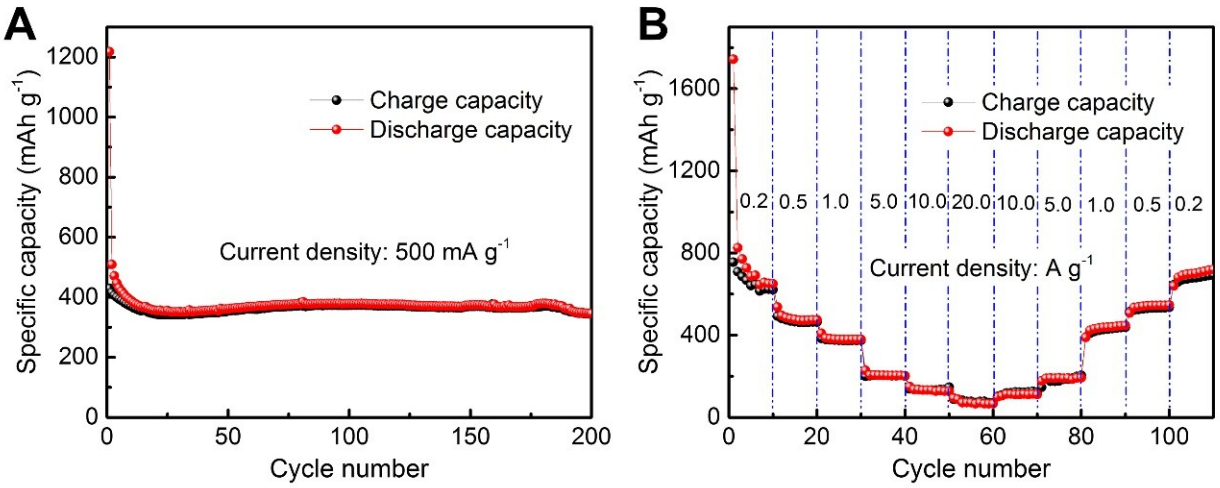

Figure S12. Cyclic stability (A) and rate capability (B) of pure CMK-3.

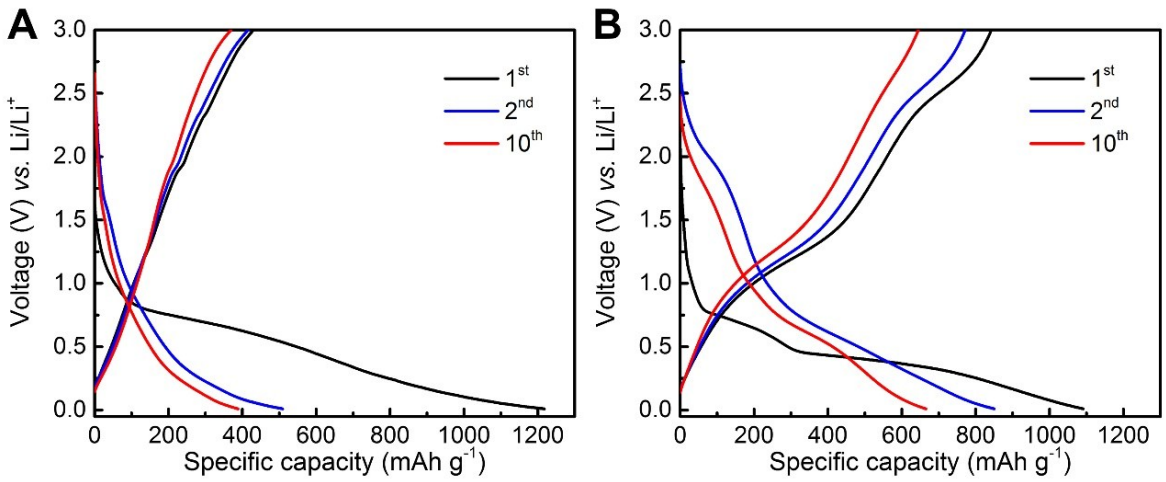

Figure S13. Charge/discharge voltage profiles of (A) pure CMK-3 and (B) $Ni_3V_2O_8$ aggregates.

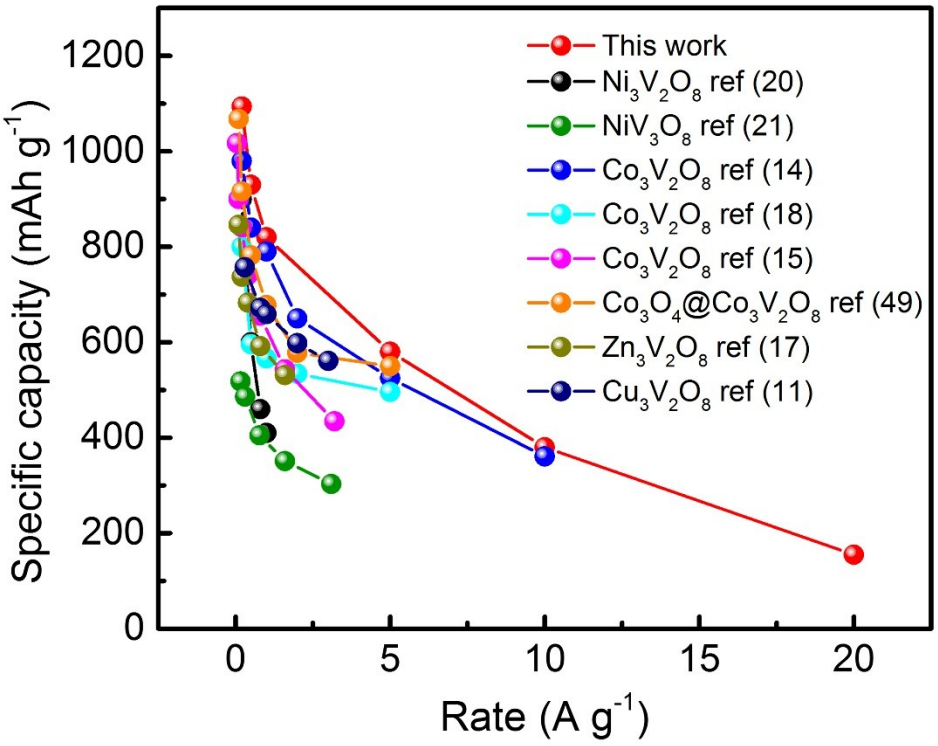

Figure S14. Comparison of rate performance with other ternary metal vanadates for LIBs.

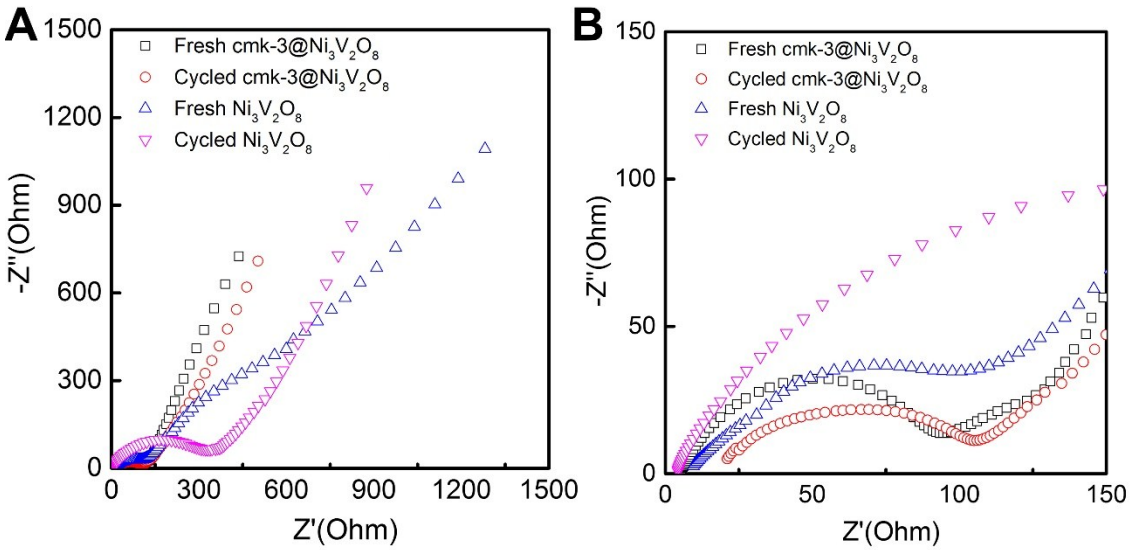

Figure S15. Full part (A) and amplified part (B) Nyquist plots of $Ni_3V_2O_8$@CMK-3 and pristine $Ni_3V_2O_8$ aggregates electrodes in fresh states and states after 100 cycles measured with an amplitude of 5.0 mV over the frequency range of 100 kHz and 0.01 Hz by applying a sine wave.